Catalysis Today 413-415 (2023) 113969

Contents lists available at ScienceDirect

Catalysis Today

journal homepage: www.elsevier.com/locate/cattod

Toward a facile depolymerization of alkaline lignin into high-value platform chemicals via the synergetic combination of mechanocatalysis with photocatalysis or Fenton process

Dominic Aboagye, Francesc Medina, Sandra Contreras *

Departament d'Enginyeria Química, Universitat Rovira i Virgili, Av. Països Catalans, 26, 43007 Tarragona, Spain

ARTICLE INFO

Keywords:
Lignin depolymerization
High-value chemicals
Mechanocatalysis
Photocatalysis
Fenton

ABSTRACT

Even though lignin is very rich in aromatic compounds, it remains the least exploited fraction of biomass due to its recalcitrant nature. Consequently, prevailing efforts to fully unlock its potential are still far from reaching due to the use of harsh conditions and energy-intensive processes which are not environmentally friendly. Herein, a facile approach for coupling acid-catalyzed mechanocatalysis (MC) via ball milling with TiO_2 photocatalysis (PC)/Fenton for depolymerization of alkaline lignin was investigated. Mechanocatalysis (MC) involved prior acid impregnation (AI) followed by ball milling. A direct comparison of pretreatments (AI, BM, MC) coupled with oxidation processes was preliminarily undertaken. The untreated lignin (UL) served as the control. MC/PC showed the highest yield of major aromatic products. Vanillin, homovanillic acid, acetovanillone, guaiacol, and vanillic acid were major aromatic building blocks identified and quantified. Further optimization revealed a total monomer yield of 22.77 wt%. SEM and FTIR analysis were done with the latter revealing the existence of pre-oxidation reaction in the BM and MC lignin prior to PC. The proposed synergetic process could offer an advantage over prevailing robust systems used for lignin depolymerization.

1. Introduction

The long-term sustainability of future biorefinery cannot be possible without full utilization of lignocellulosic biomass. Lignin constitutes 15–30 wt% of lignocellulosic biomass [1,2]. It is considered the largest source of aromatic building blocks, thereby making its depolymerization one of the most highly attractive options [3,4]. However, lignin remains underutilized compared with the carbohydrate fraction of biomass. Of the over 70 million tons of lignin industrially produced, approximately 98% is burnt for energy or disposed into landfills causing environmental threats, with only 2% utilized for value-added chemicals production [1,2].

As a 3-dimensional aromatic polymer, lignin is made of three monolignols, namely coniferyl alcohol, p-coumaryl alcohol, and sinapyl alcohol. The structural units result in the formation of C-C and C-O-C bonds such as alkyl-alkyl, alkyl-aryl, and aryl-aryl interlinkages [5,6]. Depending on the nature of the plant (softwood or hardwood), the patterns of interlinkages may vary, with β-O-4 being the abundant bonds (approximately 50%). Industrially, the isolation of lignin can be done through three key techniques, such as sulfite, kraft, and organosolv processes [7]. Conventional depolymerization strategies such as hydrogenolysis, pyrolysis/gasification, hydrothermal, and chemical depolymerization have been applied to isolated lignin [8,9]. However, these processes are relatively expensive and require robust conditions, with the predominant formation of defunctionalized products (for example xylene, benzene, etc.) [10].

Recently, photocatalysis and Fenton processes have been applied widely for biomass conversion or/and organic synthesis via radical oxidation. Fenton process is a homogenous technique based on the combination of iron and H_2O_2 in an acidic medium to generate reactive oxygen species (ROSs), i.e., OH radicals. Photocatalysis is a technique that requires the use of a photocatalyst and light having energy equal or greater than the band gap of the photocatalyst. Therefore, the irradiation of the photocatalyst produces ROSs on the surface. TiO_2 is the most studied and used photocatalyst lab-scale and even on large scale due to its low cost, ubiquitous, and high efficiency[11]. Labidi and colleagues [12] applied TiO_2 for depolymerization of organosolv lignin (black liquor) and 1-Butyl-3-methylimidazolium methyl sulphate ([Bmim][$MeSO_4$]) ionic liquid pulping methods, under UVA irradiation and with the organosolv liquor treated with photocatalyst afforded considerable

* Corresponding author.
E-mail address: sandra.contreras@urv.cat (S. Contreras).

https://doi.org/10.1016/j.cattod.2022.11.030
Received 4 September 2022; Received in revised form 8 November 2022; Accepted 27 November 2022
Available online 2 December 2022

yield of phenolic compounds and 20% oil yield [11]. To date, the sole application of PC for depolymerization lignin to aromatic compounds has not been fully effective. Innovatively combining other green technologies to produce lignin-derived platform chemicals could be promising [13]. Notably, a high yield of phenolic monomers during depolymerization of lignin must be pretreated before the application of the depolymerization strategy [14].

Different pretreatments (chemical, biological and mechanical) techniques have been developed for biomass, and the outcomes indicate that they could enhance depolymerization[15–18]. Sturgeon et al. [16] via a mechanistic study involved in the cleavage of β-O-4 bond in four model compounds in the presence of H_2SO_4 at 150 °C reported high cleavage of interlinkages and indicated that the prevalence of methoxy group on phenyl ring determines the distribution of products. Tayier and colleagues [19] studied the catalytic effect of various acids, including H_2SO_4, HCl, formic acid, and H_3PO_4, under microwave-assisted conditions at 160 °C for lignin depolymerization. Interestingly, H_2SO_4 and formic acid afforded the highest production of lower molecular weight compounds. Rahimi et al. [20] reported more than 60 wt% yields of aromatic monomers via the depolymerization of lignin in aqueous formic acid. Notwithstanding the progress made, these studies have primarily been conducted at significantly high temperatures.

Over recent years, mechanochemical techniques have been applied to initiate and modify chemical transformations, particularly in organic synthesis [23]. Mechanochemistry has been predicted to promote pre-oxidation of lignin via direct cleavage of β-O-4 interlinkages, hence lowering further the lignin deconstruction reaction barrier via acid-catalyzed mechanical activation [21,22]. Hence, coupling lignin pretreatment using mechanocatalysis (MC) and depolymerization via Fenton/photocatalysis could be promising and this has not been a subject of a more thorough examination [13].

Inspired by recent mechanochemistry and advanced oxidation process applications, we investigated the synergistic effect of coupling untreated lignin and pretreated lignin (AI alone, BM alone, and MC) with Fenton/photocatalysis on the yield and distribution of aromatic building blocks from alkali lignin. Based on the preliminary findings, process parameters will be optimized to maximize performance. The effect of these treatments and oxidation strategy on the structure and morphology of lignin will be analyzed.

2. Materials and methods

2.1. Chemicals and materials

Alkaline lignin(L0082) was purchased from TCI Chemical Reagent. Before each reaction, the lignin sample was oven dried at 40°C for 24 h. Various major phenolic monomers such as guaiacol (99%), 99% vanillin (4-hydroxy-3-methoxybenzaldehyde), acetovanillone (99%), homovanillic acid (99%), vanillic acid (99%), used for GC calibration were purchased from Sigma-Aldrich®. Other reagents include 30% (w/w) H_2O_2, H_2SO_4(96%), NaOH (>98%), $FeSO_4{\cdot}7\ H_2O$ (≥99.0%), and Aeroxide® P25 TiO_2 were purchased from Sigma-Aldrich® and Alfa Aesar. The schematic representation of the method used is also shown in the supplementary data (Fig. S1).

2.2. Lignin pretreatment

2.2.1. Acid impregnation (AI)

The acid-impregnation strategy adopted in this study was inspired by previous works [23,24], with minor modifications. Briefly, 4 g of alkali lignin was suspended in 75 mL of diethyl ether containing 1.5 mmol H_2SO_4 per gram of lignin and stirred continuously for 2 h. A rotary evaporator was used to evaporate the diethyl ether at 40 °C, successfully recovering both the solvent and lignin. If not used immediately, the AI was kept in a fridge at − 4 °C for later use.

2.2.2. Ball milling (BM) and mechanocatalysis (MC)

Acid-catalyzed ball milling (MC) pretreatment and BM of the untreated lignin (UL) were done in a planetary ball mill (Fritsch, Pulverisette P7) having an 80 mL jar. The jar was equipped with five milling balls (10 mm diameter, stainless steel). Ball milling conditions were adopted from a previous study [24] with slight modification. Briefly, 2 g of either AI lignin or UL was loaded into the jar. During the milling process, a speed of 600 rpm, a milling time of 60 mins, and four cycles of 15 mins run and 10 mins pause time were used.

2.3. Photocatalytic and Fenton lignin depolymerization

For our preliminary experiments, the untreated lignin (UL) and pretreated lignin (AI) including BM, AI alone and MC alone were oxidized using either photocatalysis (Lignin=8 g/L, TiO_2 =1 g/L, Time=60 mins, unaltered initial pH=9.6) or Fenton (Lignin=8 g/L, H_2O_2 =1 g/L, Time=60 mins, Fe^{2+}=0.2 g/L, pH=3.0). The system recording the highest yield of phenolic monomers was selected and taken through subsequent process optimization.

2.3.1. Fenton lignin depolymerization

A 100-mL round bottom Erlenmeyer flask was used as the reactor. Lignin (8 g/L) was weighed, and 20 mL of water was added. $FeSO_4{\cdot}7\ H_2O$ was weighed and dissolved in the mixture to obtain an Fe^{2+} concentration of 0.2 g/L. Afterward, the pH of the mixture was adjusted to 3.00 ± 0.05 using 2 M H_2SO_4. Subsequently, H_2O_2 (1 g/L) was added to initiate the reaction for 60 mins. The aqueous phase after the reaction was extracted using ethyl acetate three times. GC/MS and GC/FID were used for liquid product identification and quantification, respectively. All batch experiments were conducted in duplicate.

2.3.2. Photocatalysis lignin depolymerization

For the photocatalytic reaction, a 100 mL borosilicate round bottom flask was used as the reactor to perform photocatalytic lignin depolymerization. The flask was placed in a SUNTEST CPS+ solar simulator with an UV range of 300–400 nm. Unlike the preliminary study with fixed conditions, the PC parameters were varied: lignin (2–16 g/L), TiO_2 (0.5–4 g/L), and pH (5−11). A 20 mL of lignin solution was prepared and loaded with an appropriate dose of the TiO_2 photocatalyst. Initially, the reaction mixture was kept under constant stirring for 15 mins in the dark for the attainment of adsorption-desorption equilibrium. The light intensity was 250 W/m^2. Sampling was done and filtered via a 0.22 μm PTFE filter. The aqueous phase after sampling was extracted three times using ethyl acetate and evaporated under vacuum. GC/MS and GC/FID were used for liquid product identification and quantification, respectively. The solids in the aqueous phase were precipitated using 4%(v/v) H_2SO_4, recovered through centrifugation, dried, weighed, and subsequently used for the solid analysis. All batch experiments were conducted in duplicate.

2.4. Product characterization

2.4.1. Identification and quantification of liquid products

The extracted organic phase from each reaction was identified and quantified using GC/MS and GC/FID, respectively. The GC was performed using a Shimadzu GC QP2010 equipped with a capillary column (ZB-WaxPlus™, 30 m x 0.25 mm i.d., 0.25 μm). Further details of GC-MS and GC-FID programmed conditions are provided in supplementary data (Section 1.1). The following Eqs. (1 and 2) were used to compute the yield of liquid products and conversion of lignin, respectively:

$$\textit{Phenolic monomer yield}\ (wt\%) = \frac{M_{compound}}{M_{initial}} x100 \quad (1)$$

$$\textit{Lignin conversion}\ (\%) = \frac{M_{initial} - M_{final}}{M_{initial}} x100 \quad (2)$$

where $M_{compound}$, $M_{initial}$ and M_{final} depict the mass of the obtained aromatic compound(g), the initial weight of lignin(g), and the weight of lignin(g) after reaction, respectively.

2.4.2. Total organic carbon analysis

The total organic carbon (TOC) of the aqueous phase was analyzed using a Shimadzu TOC analyzer. We examined the variation of available carbon by assessing the overall conversion of carbon ($TOC_{overall}$) from initial TOC ($TOC_{initial}$) and the percentage of $TOC_{overall}$ converted to aromatics ($TOC_{aromatics}$). It is important to note that the TOC after reaction in the aqueous phase ($TOC_{aqueous}$) was measured after ethyl acetate extraction. The following Eqs. (3-5) were used to compute and elucidate carbon flow:

$$TOC_{overall} = \mathrm{TOC}_{initial} - \mathrm{TOC}_{aqueous} \quad (3)$$

$$TOC_{overall}(\%) = \frac{\mathrm{TOC}_{initial} - \mathrm{TOC}_{aqueous}}{\mathrm{TOC}_{initial}} \mathrm{x}100 \quad (4)$$

$$TOC_{aromatic}(\%) = \frac{(\text{number of carbons in monomer})(\text{concentration of monomer})}{\text{Initial TOC}} \mathrm{x}100 \quad (5)$$

where $TOC_{initial}$, $TOC_{overall}$, $TOC_{aqueous}$, and $TOC_{aromatic}$ depict the initial TOC in aqueous before Fenton/photocatalysis reaction, overall TOC converted, TOC remaining in the aqueous phase after reaction, and percentage of overall TOC which resulted in the formation of aromatics, respectively.

2.4.3. Lignin characterization

The UL, lignin remaining after pretreatment, and obtained oxidized lignin were analyzed using Environmental scanning electron microscopy (ESEM) and Fourier-transform infrared spectroscopy (FT-IR). The FT-IR spectra were analyzed in the region of 4000–500 cm^{-1} with an attenuated total reflectance (ATR) cell using a 4/cm resolution.

3. Results and discussion

3.1. Preliminary screening of pretreatments coupled with PC/Fenton

Fig. 1 shows the effect of the different pretreatments (AI, BM alone, and MC) on the yield and distribution of phenolic monomers when coupled with PC or Fenton. UL coupled with PC or Fenton served as a control. Monomers such as guaiacol, vanillin, acetovanillone, homovanillic acid, and vanillic acid (significantly present only in MC/PC) were major aromatic products found. The GC/MS profile of all products found are presented in supplementary data (Fig. S2 and Table S1).

As shown, the yields of 0.02 and 0.06 wt% in UL and AI were respectively obtained when coupled with Fenton, and the coupled PC systems resulted in yields of 0.017 and 0.29 wt% in UL and AI, respectively. From the GC/FID (Fig. 1), MC/PC treatment afforded the maximum yield of total monomeric compounds 987.01 mg/L (corresponding to 12.33 wt%) compared with UL, BM and AL when coupled with Fenton depolymerization. The maximum yield of individual phenolics occurred in the MC/PC system and followed the trend: vanillin (5.97 wt%) > acetovanillone (2.78 wt%) > guaiacol (2.36 wt%)

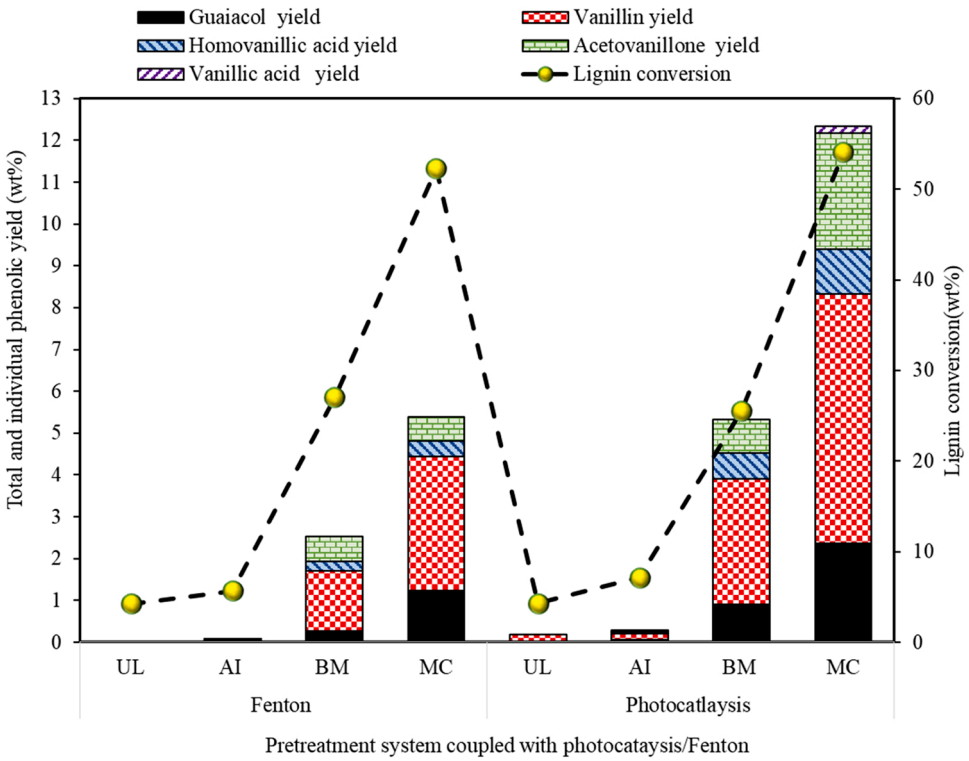

Fig. 1. Relative yields of major phenolic aromatic monomers were tested over different pretreatment conditions. PC conditions (Lignin=8 g/L, TiO_2 =1 g/L, Time=60 mins) and Fenton (Lignin=8 g/L, H_2O_2 =1 g/L, Time=60 mins, Fe^{2+}=0.2 g/L) were used.

> homovanillic acid (1.07 wt%). BM/PC recorded the next highest performance (yield of 5.34 wt% and concentration of 426.86 mg/L). Correspondingly, the maximum conversion of lignin (54.07 wt%) was achieved in the MC/PC system and 52.25 wt% in the MC/Fenton. Conversions of the UL and AI lignin coupled with photocatalysis were significantly low. To understand the contribution of the catalytic processes (Fenton/PC), each pretreated sample (UL, AI, BM, MC) was dissolved in the same quantity of solvent used for Fenton/photocatalysis, extracted and analyzed without coupling the Fenton/PCs reactions. The results showed traces of monomer, with yields of 0.001 wt%, 0.001 wt %, 0.003 wt% and 0.004 wt% in the UL, AI, BM and MC, respectively (Fig. S3).

The low yields of total monomeric compounds detected in Fenton/PC oxidation of UL and AI lignin could potentially be due to the inability of the radicals to effectively attack and dissociate the interlinkages owed to the large molecular weight of lignin. Hence, we speculate that the monomers obtained could have prevailed inherently in the lignin sample probably during isolation. This conclusion agrees with observations made in another study [14] and also the low traces of monomeric compounds found in the pretreated samples without Fenton/PC

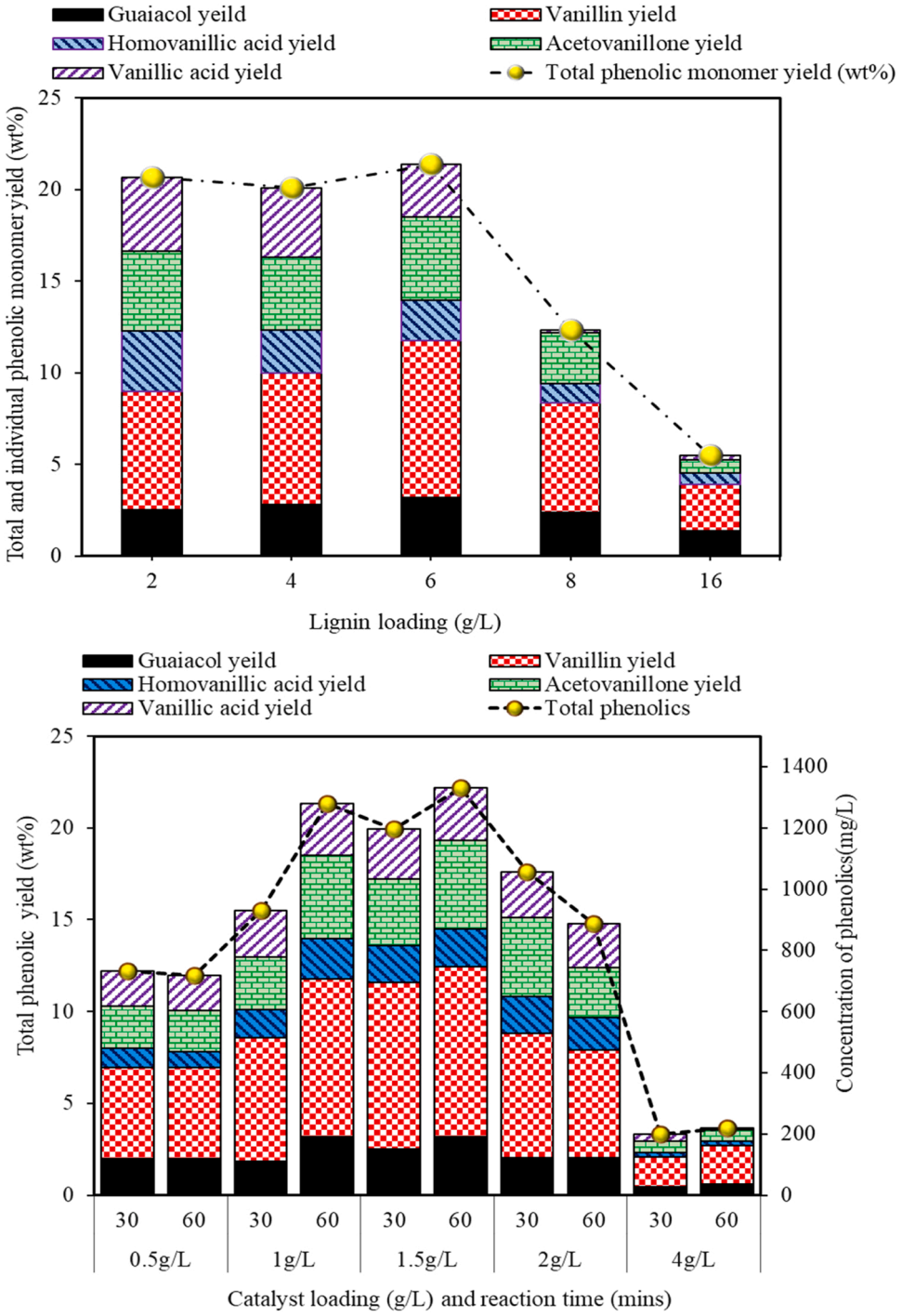

Fig. 2. Effect of photocatalytic conditions on the yield of phenolic monomers in MC/PC system. (a) lignin loading (2–16 g/L) at fixed PC conditions (TiO_2 = 1 g/L, unaltered initial pH = 9.6 and time =60 min). (b) TiO_2 loading (0.5–4 g/L) and time (30 and 60 min) at fixed PC conditions (lignin loading = 6 g/L, unaltered initial pH = 9.6).

(Fig. S3). However, these yields were improved in BM or MC lignin when coupled with photocatalysis. Nair et al. [14] demonstrated the feasibility of wet ball milling (acetone and water mixture) of lignin with TiO_2 mixtures affording phenolic monomers and aromatic hydrocarbons. They detected almost similar types of monomers present in our liquid samples. However, the proposed coupled MC/PC system in this study afforded higher yields of these monomers. First, we speculate that the application of H_2SO_4-catalyzed ball milling could likely have promoted the availability of highly oxidative precursors, hence a possible occurrence of pre-oxidation. Pre-oxidation could lower the bond dissociation energy of the C–O bond, hence making β–O–4 linkage highly labile [22]. Our preliminary results showed a lower yield of monomers in the Fenton reaction compared to PC reactions. The low yield in Fenton as compared to PC could be ascribed to the possibility of further conversion of products to undesired ring open products or further oxidation via reactivity of phenolic motifs. Previous studies speculated that Fenton reactions may facilitate the formation of ring open chemicals [25,26]. This explanation may not be supported by the results since the conversion of lignin was not significantly different between MC/PC and MC/Fenton (Fig. 1). However, this interesting observation agrees with the study by Du and colleagues [31] where a higher lignin conversion but lower yields of aromatic compounds was record in the system with $Bi_2TiO_4F_2$ as photocatalyst but vice versa using C_{60}/TiO_2 as photocatalyst. It is therefore reasonable to indicate that high lignin conversion may not always correlate with yield of aromatic products, and that aromatic product accumulation in each system (Fenton or PC) and substrates may respond differently to reactive species. Enlightened by the relatively superior performance of the MC/PC system compared to the Fenton coupling strategies, we optimized various factors affecting photocatalysis reactions.

3.2. Effect of photocatalysis operating conditions on the performance of MC/PC

3.2.1. Effect of lignin loading

Generally, there is a lignin concentration threshold such that, once exceeded or unreached, the photocatalytic activity may be negatively affected [27]. Fig. 2a shows the effect of lignin loading (2–16 g/L) on PC. A maximum yield of 21.35 wt% of total aromatic monomers was obtained in the system with 6 g/L lignin loading with the following trend in individual monomers: vanillin (8.59 wt%)> acetovanillone > (4.55 wt%) > guaiacol (3.18 wt%) > homovanillic acid (2.85 wt%) > vanillic acid (2.19 wt%). Overall, we observed an almost constant yield of total aromatic monomer with lignin loading from 2 to 4 g/L, a slight increase from 4 to 6 g/L and a sharp decline in yield when loading exceeds 6 g/L. Compared with our preliminary study where lignin loading of 8 g/L was used, lowering the lignin loading to 6 g/L led to 1.73x increase in the yield of total monomers (from 12.34 to 21.35 wt %).

Previous reports have shown that low concentrations of lignin facilitate strong interactions between the catalyst and photonic flux irradiated thereby increasing ($^{\bullet}OH$) radical formation during PC [28]. Du et al. [29] applied C_{60}-modified $Bi_2TiO_4F_2$ photocatalyst for depolymerization of pine kraft lignin and observed a reduction in the yield of monomers when the concentration of the initial lignin substrate was increased. They ascribed this reduction to two main reasons: thus, the low transmittance of irradiated light, and the significantly higher lignin adsorption onto the catalysts' surface when the concentration of lignin was increased. Nguyen [30] reported low yield of monomers in batch reactors at high lignin loading, however, these yields could significantly be increased in a continuous flow reactor which demonstrated to some extent yield of both 4′-methoxyacetophenone and guaiacol under high lignosulfonate lignin loading and low transmittance. Overall, lignin loading has clearly shown to affect light absorption, especially in batch reactors, which was more evident in the yield at loading above the optimum, thus 6 g/L.

3.2.2. Effect of catalyst loading

Likewise, the appropriate selection of catalyst amount could play an important role in photocatalysis reactions[31]. Fig. 2b depicts the yield, distribution, and concentration profiles of monomers at varying catalyst loading (0.5–4 g/L) and time (30 and 60 mins). Though there was a continuous increase in yield and concentration in systems having 0.5 g/L and 1.5 g/L, we observed a drop in performance as catalyst loading was increased to 2 g/L and 4 g/L. The maximum total monomers yield was 22.20 wt% and this occurred at 1.5 g/L catalyst loading, while the individual phenolics followed the trend: vanillin (9.26 wt%)> acetovanillone (4.83 wt%) > guaiacol (wt%)> homovanillic acid (2.88 wt%) > vanillic acid (2.05 wt%). Compared with the preliminary investigation, increasing the catalyst loading from 1 to 1.5 g/L and reducing lignin loading from 8 to 6 g/L, increased the total monomer yield 1.77x.

The reduction in performance at high catalyst loading (4 g/L) could be attributed to a possible overoxidation of phenolic products at high catalyst loading [25,31]. With illumination time showing a great effect on yield, previous reports have also noted that 60 mins exposure was optimal for maximum yields [12,31]. Different researchers have reported varying results on the influence of catalyst concentration. Kansal and colleagues [27] investigated the effect of varying ZnO doses (0.5–2 g/L) on Kraft lignin solutions. There was an increase in performance from 0.5 to 1 g/L (due to increasing catalyst active sites) with 1 g/L being the optimum concentration [38]. In contrast to this, a catalyst concentration of 2 g/L has been reported as the threshold value for optimum photocatalysis activity[32]. The difference in thresholds reported in the literature could be speculated to be the interplay of factors (solute loading and catalyst loading). Reideh [33] explained this by indicating that initial solute concentration determines the optimum catalyst loading since inappropriate loading could affect the overall active sites available on the catalyst surface.

3.2.3. Effect of pH

Also, pH does affect photocatalytic reactions[29]. The role of pH (5−11) and time (30–180 mins) on the yield and product distribution of monomers are shown in Fig. 3. From the results, all systems showed increasing yields over different pH (5, 8 and 11) from 30 to 60 mins, and a decreasing trend as treatment time exceeds 60 mins. Correspondingly, the sample treated at pH of 8 showed maximum yields, followed by pH 11, with treatments conducted at pH of 5 affording the least performance as shown in Fig. 3(a-c). Overall, the yields obtained were 1075.73 mg/L (17.92 wt%), 1366.39 mg/L (22.77 wt%), 1148.85 mg/L (19.14 wt%) for pH 5, 8 and 11, respectively as shown in Fig. 3(d).

The reduction in monomers over extended irradiation time in all systems is possibly due to overoxidation but also repolymerization of the monomers back into dimers/oligomers. Typically, depolymerization and/or repolymerization occur simultaneously depolymerization of lignin [34,35]. The maximum yield was obtained in the system treated at pH of 8 but decreased at a pH of 11. This could be due to the interaction of different factors such as alteration of catalyst properties, which is principally related to the acid-base equilibrium of adsorbed OH-group [36]. Additionally, excessive conversion of phenolic motifs at high pH with an almost complete degradation of Kraft lignin at pH of 11.6 have been reported by Villasenor and Mansilla [37]. At pH= 5, the yields were low as compared to 8 and 11. Acid pH could also result in lignin precipitation, hence low performance.

Gong and colleagues [31] also reported a reduction in product yield during photo-depolymerization of lignin at low pH and indicated that high pH results in an increased production of OH radicals. Another plausible explanation could be due to increased adsorption of some of the products and lignin onto the surface of the catalyst when the pH decreases lower than the point of zero charge of the catalyst, while at basic pH the variation of charges present on the catalysts' surface might also repel leading to high yields [38]. The point of zero-point charge of the TiO_2 P25 used is 6.25. Gong and colleagues [31] also associated the

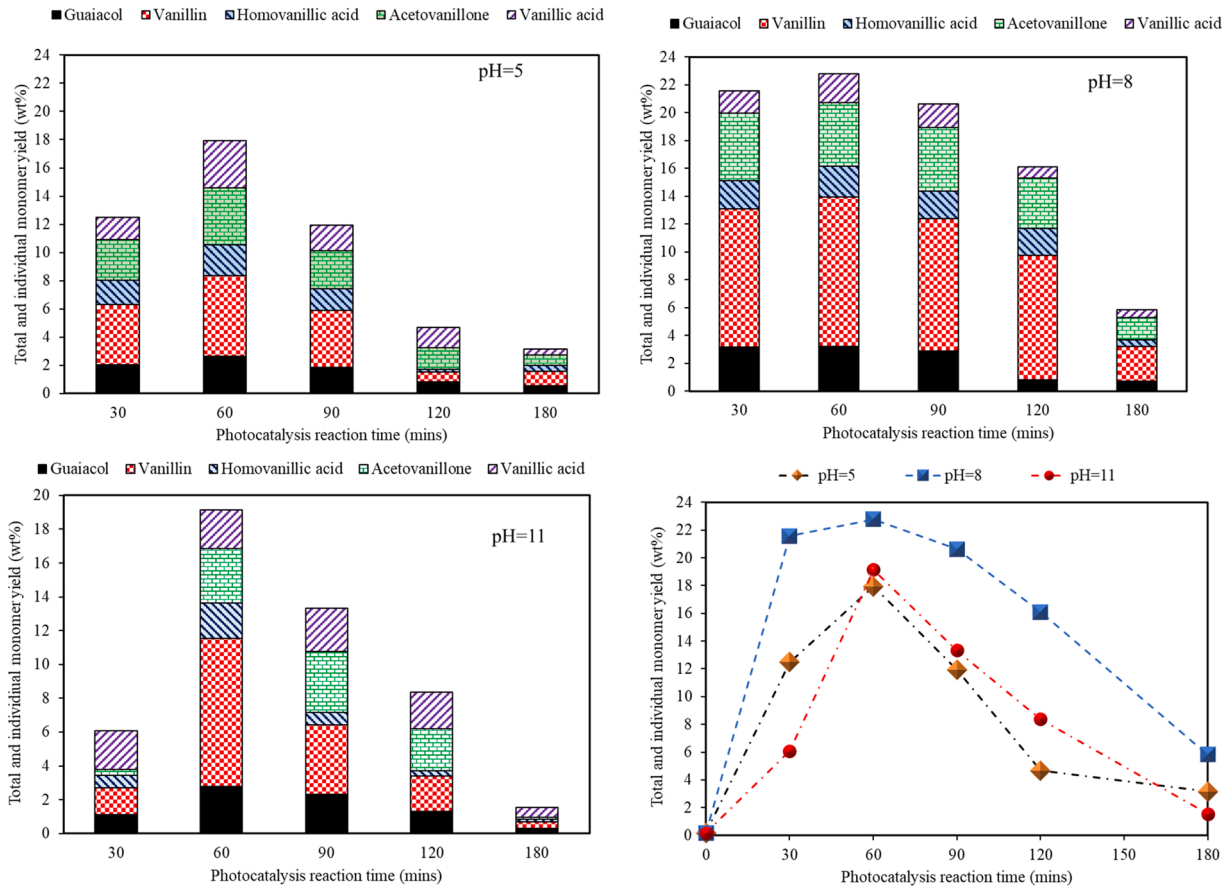

Fig. 3. Influence of pH (5,8,11) and time (0–180 mins) on phenolic product yield in the MC/PC system. (a) pH = 5, (b) pH = 8, (c) pH = 11, (d) compared (pH 5,8 and 11). PC conditions (lignin loading = 6 g/L, TiO_2 = 1.5 g/L).

low depolymerization performance at acidic pH to the increase adsorption of lignin to the surface of catalyst.

3.3. Elucidating carbon variation in the proposed MC/PC system

We further examined the TOC variation in the MC/PC system, over the different pH (5, 8, 11) under the other optimal conditions. This was primarily done to understand the proportion of available TOC which were effectively converted to phenolic monomers and or other compounds/mineralized/repolymerized. Table S3 shows the results for the overall TOC converted ($TOC_{overall}$) which was computed using Eqs. (3) & (4), and TOC converted to aromatics monomers (thus $TOC_{aromatics}$) was computed using Eq. (5).

The results of TOC showed that, of the 3789.7 mg/L $TOC_{initial}$ in the aqueous solution before reaction, 699.45 mg/L (18.46%) represented $TOC_{overall}$ with 17.59% effectively converted to $TOC_{aromatics}$ at pH= 5. As expected, significantly high $TOC_{overall}$ was observed in samples treated at pH= 8 and pH= 11, with the samples treated at pH 11 being the highest. The difference in $TOC_{overall}$ and $TOC_{aromatics}$, thus TOC converted to other unidentified products or mineralized, were 32.95 mg/L (0.87%) for pH= 5, 159.70 mg/L (4.21%) for pH= 8 and 267.25 mg/L (7.05%) for pH= 11.

The TOC analysis is in direct correlation with the pH studies in the preceding section with pH= 5 recording the least yield. The reaction at pH= 5 indicated the least difference between $TOC_{overall}$ and $TOC_{aromatics}$, hence low possibility of mineralization/ring open-compound formation. This emphasizes the effect of decreased solubility of lignin at acidic pH. It is worth noting that though there existed no significant difference between the $TOC_{overall}$ for MC/PC treated at pH= 8 and 11, the TOC $_{aromatics}$ were significantly different with about 7.05% of $TOC_{overall}$ not converted to $TOC_{aromatics}$ at pH= 11. This could likely confirm an indication of either ring open or mineralization at pH= 11 [37,39]. Therefore, it could be assumed that some phenolic products, particularly for samples handled at higher pH, may have further reacted, and swiftly decomposed into other products.

3.4. Characterization of solid products

3.4.1. SEM analysis

The effect of pretreatment and MC/PC lignin on the morphology of lignin were tracked using SEM graphs (Fig. 4). From Fig. 4a, the UL possessed large round-shaped particles with some large-sized cracked particles. Similarly, the SEM of AI lignin is depicted in Fig. 4b. The shape of UL particles and AI were relatively large, with the AI samples showing more holes between the particles compared to UL samples. The BM lignin (Fig. 4c), MC (Fig. 4d) and the MC/PC lignin (Fig. 4e) showed small, rounded morphology of particles with the MC/PC samples showing the least sized particles compared to UL and AI samples. The small size and shapes of the mechanically pretreated samples is ascribed to heat generation during the process and impact of mechanical forces on samples [40,41].

3.4.2. FT-IR spectra analysis

FTIR spectra for the UL, AI, BM, MC, and MC/PC lignin are compared and presented in Fig. 5. The presence of carbonyl, hydroxyl, methoxy, and aromatic rings from FTIR spectra were analyzed following a previous report for the identification of lignin functional groups, as summarized in the peak assignment in Table S3 [17]. The prevalence of phenolic –OH (3385 cm-1) stretch decreased in BM, MC, and MC/PC, indicating the removal of hydroxyl, with high abundance in UL and AI

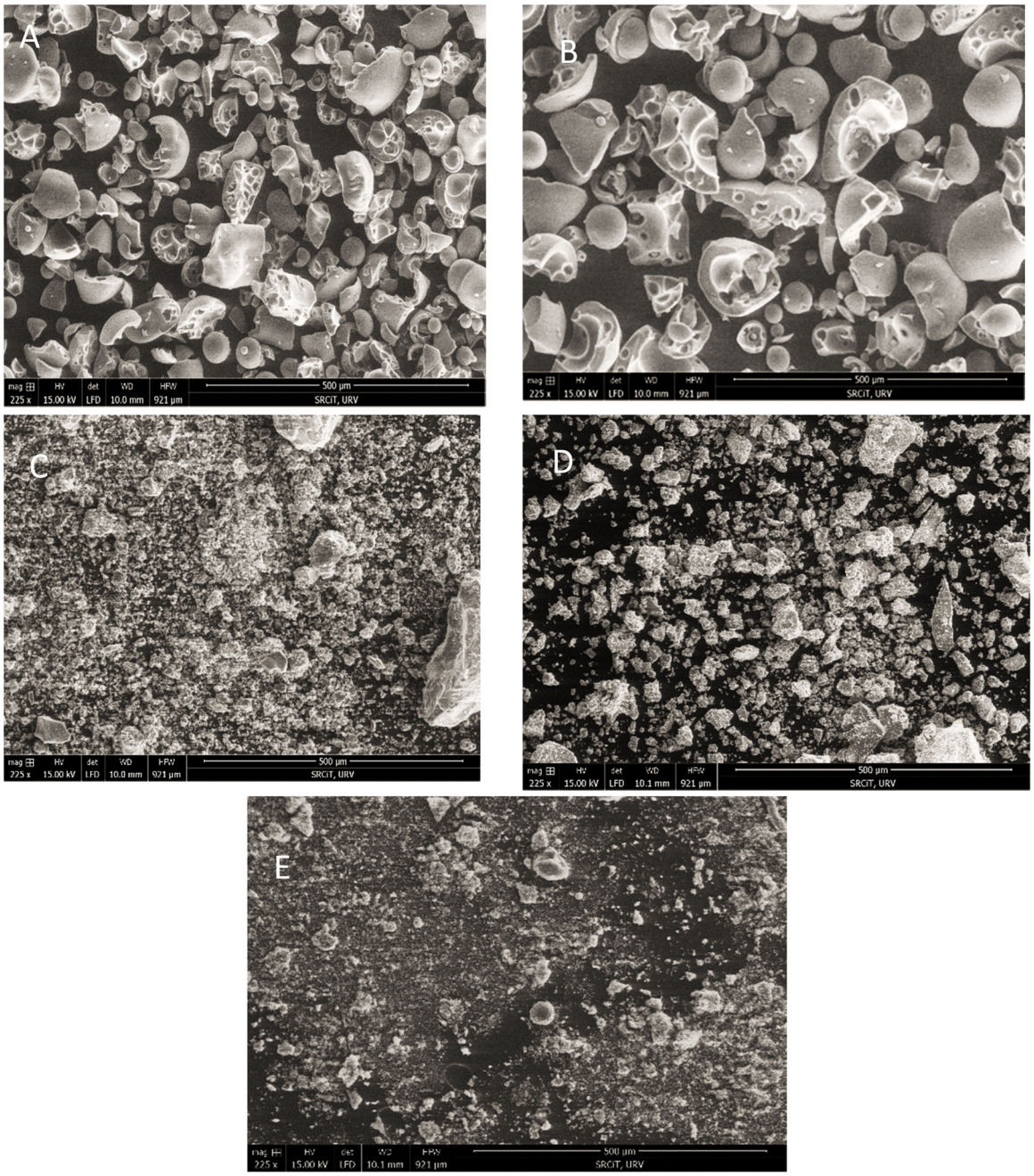

Fig. 4. SEM of alkaline lignin: (a) UL (b) AI lignin, (c) BM lignin, (d) MC lignin, and (e) MC/PC lignin.

samples.

The decreasing intensity of asymmetric aliphatic C−H (2925 cm-1) deformations suggested a possible prevalence of demethylation and demethoxylation reaction of lignin, especially in MC/PC lignin [42]. Many distinct absorption bands appeared in the fingerprint area, between 1800 and 900 cm^{-1}. The bands for aromatic skeleton vibrations, assigned at 1596, 1510 and 1460 cm^{-1}, showed similar signal pattern in all samples which means the main structure of the aromatic ring of lignin is preserved, which is a requirement for subsequent production of aromatic compounds in lignin [40]. The Peak at 1156 cm^{-1} corresponds to the conjugated stretching vibration of ester-based C═O, while the absorption band at 1697 cm^{-1} primarily depicts C═O stretching vibrations in aldehyde/ketone groups, and the strength of these peaks demonstrated a high absorption in the UL and AI treatment, but a decrease in BM, MC, and a further reduction in MC/PC. Hence, there is reasonable evidence of the prevalence of pre-oxidation in BM and MC pretreated samples.

Additionally, moving from UL to MC/PC, the degradation of carbonyl and carboxyl groups may also occur in addition to the oxidized lignin structure. This agrees with a previous study which indicated the promotional effect of C_α alcohol oxidation to ketone on the cleavage of β-O-4 linkages, and the destruction of conjugated carbonyl structure remains the main mechanism associated with depolymerization of lignin under acidic pretreatment [20]. The MC alone and coupled MC/PC lignin has a lower relative amount of hydroxyl and methoxy groups (1326, and 1115 cm^{-1}), demonstrating once more that the oxygen-containing groups, ether linkages, and other side chains are cleaved most quickly. The guaiacyl units connected to the band at 1030 cm^{-1} represent –CH plane deformation in guaiacyl and C-O deformation in primary alcohols. These peaks were weak in MC and depolymerized lignin compared to other treatments, indicating that many guaiacyl units were cleaved. Intensive ball milling could influence

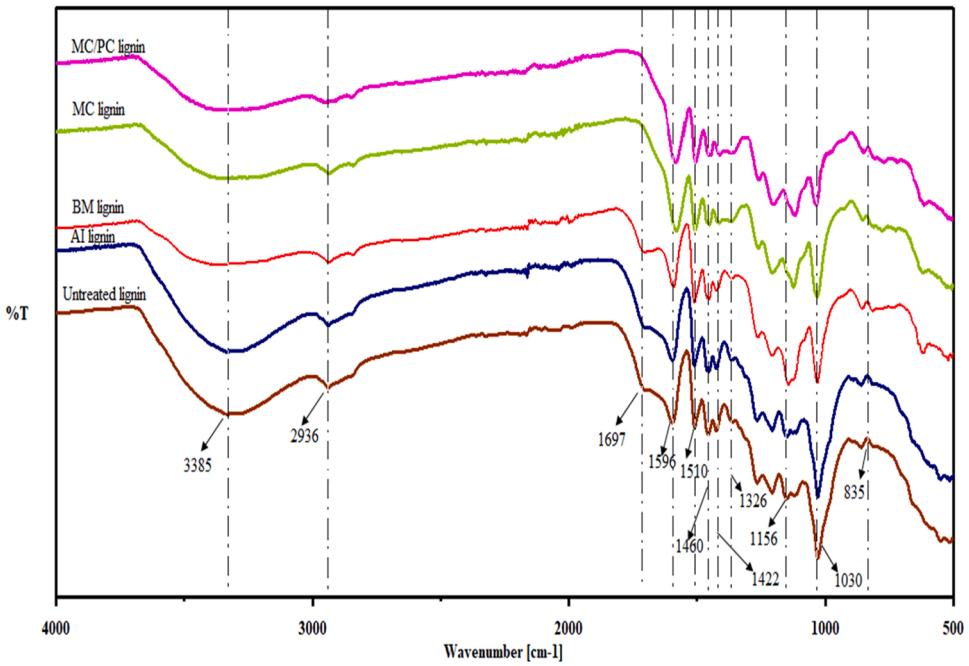

Fig. 5. ATR-FTIR spectra of alkali lignin for UL, pretreated lignin, and unconverted MC/PC lignin.

the pre-oxidation of β-O-4 bonds in lignin and decrease the molecular weight prior to PC [22,43], hence the high performance in pretreated samples. Overall, the FTIR spectra showed clear modifications in lignin chemical structure especially during MC and MC/PC, which were advantageous for breaking ether linkages in lignin. Hence, enhanced performance in these systems compared to UL, AI and BM samples. As reported in the preliminary assessment (Fig. S3), the samples pretreated with MC did not show high yields of phenolic monomers as compared with the coupled MC/PC. However, the FT-IR showed that MC pretreated lignin were pre-oxidized. Mechanistically, via the systematic MC and PC two-step process, the MC process pre-oxidized primary/secondary alcohols available in the backbone of alkaline lignin which enables subsequent cleavage of C-O aryl bonds or other bonds available in the lignin aromatic units by the photoproduced radicals from the photocatalytic process (PC) which then forms the phenolic monomers. This has also been reported in studies using model lignin [30,44,45].

4. Conclusions

We offer a simple and environmentally benign strategy of coupling H_2SO_4-catalyzed mechanocatalysis pretreatment with radical-mediated photocatalysis/Fenton for depolymerization of lignin to aromatic building blocks. Compared to AI alone or BM pretreatments, and coupled Fenton oxidation, MC/PC exhibits superior performance towards the yield and distribution of aromatic building blocks. Vanillin, homovanillic acid, acetovanillone, and guaiacol were major platform chemicals identified. Moreover, vanillin was highly predominant than the other major products. Meanwhile, TiO_2 photocatalyst loading above 1.5 g/L, lignin loading above 6 g/L, reaction time above 60 mins, and pH above/below 8.0 result in a decline in product yield and overall depolymerization efficiency during photocatalysis reaction. Overall, the total phenolic monomer yield was 22.77 wt%. FTIR showed that pre-oxidation in the BM and MC lignin enhances PC monomer yield. TOC profiles showed a possible prevalence of over-depolymerization/undesired product formation at elevated pH of 11. Overall, the proposed synergetic process could offer an advantage over prevailing robust systems used for lignin depolymerization. Furthermore, in-depth understanding of the mechanisms involved in the mechanocatalytic process may be needed.

CRediT authorship contribution statement

Dominic Aboagye: Conceptualization, Investigation, Data curation, Formal analysis, Resources, Writing – original draft, Writing – review & editing. **Francesc Medina:** Funding acquisition, Resources, Supervision, Writing – review & editing. **Sandra Contreras:** Conceptualization, Methodology, Formal analysis, Funding acquisition, Resources, Supervision, Writing – review & editing.

Declaration of Competing Interest

The authors declare that they have no known competing financial interests or personal relationships that could have appeared to influence the work reported in this paper.

Data availability

Data will be made available on request.

Acknowledgements

Dominic Aboagye is grateful for the support from Universitat Rovira i Virgili Marti Franques Grant No. 2019 PMF-PIPF-15. This work was supported by Diputació de Tarragona (Reference number 2021/03) and Proyectos de Generación de Conocimiento AEI/MCIN (PID2021-123665OB-I00).

Appendix A. Supporting information

Supplementary data associated with this article can be found in the online version at doi:10.1016/j.cattod.2022.11.030.

References

[1] Z. Strassberger, S. Tanase, G. Rothenberg, The pros and cons of lignin valorisation in an integrated biorefinery, RSC Adv. 4 (2014), https://doi.org/10.1039/c4ra04747h.
[2] R. Roy, B. Jadhav, M.S. Rahman, D.E. Raynie, Characterization of residue from catalytic hydrothermal depolymerization of lignin, Curr. Res. Green Sustain. Chem. 4 (2021), https://doi.org/10.1016/j.crgsc.2020.100052.

[3] M. Stucchi, S. Cattaneo, A. Cappella, W. Wang, D. Wang, A. Villa, L. Prati, Catalytic oxidation of methoxy substituted benzyl alcohols as model for lignin valorisation, Catal. Today 357 (2020), https://doi.org/10.1016/j.cattod.2019.03.022.

[4] Omar Y. Abdelaziz, Ida Clemmensen, Sebastian Meier, Carina A.E. Costa, Alírio E. Rodrigues, Christian P. Hulteberg, Prof Anders Riisager, On the oxidative valorization of lignin to high-value chemicals: a critical review of opportunities and challenges, ChemSusChem (2022), https://doi.org/10.1002/cssc.202201232.

[5] V.K. Ponnusamy, D.D. Nguyen, J. Dharmaraja, S. Shobana, J.R. Banu, R. G. Saratale, S.W. Chang, G. Kumar, A review on lignin structure, pretreatments, fermentation reactions and biorefinery potential, Bioresour. Technol. 271 (2019), https://doi.org/10.1016/j.biortech.2018.09.070.

[6] Filipa M. Casimiro, Carina A.E. Costa, CarlosVega-Aguilar, Alírio E. Rodrigues, Hardwood and softwood lignins from sulfite liquors: structural characterization and valorization through depolymerization, Int. J. Biol. Macromol. 215 (2022) 272–279, https://doi.org/10.1016/j.ijbiomac.2022.06.067.

[7] F.S. Chakar, A.J. Ragauskas, Review of current and future softwood kraft lignin process chemistry, Ind. Crops Prod. 20 (2004) 131–141, https://doi.org/10.1016/j.indcrop.2004.04.016.

[8] Z. Sun, G. Bottari, A. Afanasenko, M.C.A. Stuart, P.J. Deuss, B. Fridrich, K. Barta, Complete lignocellulose conversion with integrated catalyst recycling yielding valuable aromatics and fuels, Nat. Catal. 1 (2018) 82–92, https://doi.org/10.1038/s41929-017-0007-z.

[9] W. Schutyser, T. Renders, S. van den Bosch, S.F. Koelewijn, G.T. Beckham, B. F. Sels, Chemicals from lignin: an interplay of lignocellulose fractionation, depolymerisation, and upgrading, Chem. Soc. Rev. 47 (2018) 852–908, https://doi.org/10.1039/c7cs00566k.

[10] Y. Cao, N. Wang, X. He, H.R. Li, L.N. He, Photocatalytic oxidation and subsequent hydrogenolysis of lignin β-O-4 models to aromatics promoted by in situ carbonic acid, ACS Sustain Chem. Eng. 6 (2018) 15032–15039, https://doi.org/10.1021/acssuschemeng.8b03498.

[11] R. Djellabi, R. Giannantonio, E. Falletta, C.L. Bianchi, SWOT analysis of photocatalytic materials towards large scale environmental remediation, Curr. Opin. Chem. Eng. 33 (2021), https://doi.org/10.1016/j.coche.2021.100696.

[12] R. Prado, X. Erdocia, J. Labidi, Effect of the photocatalytic activity of TiO_2 on lignin depolymerization, Chemosphere 91 (2013) 1355–1361, https://doi.org/10.1016/j.chemosphere.2013.02.008.

[13] Y. Wan, J.M. Lee, Toward value-added dicarboxylic acids from biomass derivatives via thermocatalytic conversion, ACS Catal. 11 (2021), https://doi.org/10.1021/acscatal.0c05419.

[14] V. Nair, P. Dhar, R. Vinu, Production of phenolics via photocatalysis of ball milled lignin-TiO_2 mixtures in aqueous suspension, RSC Adv. 6 (2016) 18204–18216, https://doi.org/10.1039/c5ra25954a.

[15] K. Ninomiya, K. Ochiai, M. Eguchi, K. Kuroda, Y. Tsuge, C. Ogino, T. Taima, K. Takahashi, Oxidative depolymerization potential of biorefinery lignin obtained by ionic liquid pretreatment and subsequent enzymatic saccharification of eucalyptus, Ind. Crops Prod. 111 (2018), https://doi.org/10.1016/j.indcrop.2017.10.056.

[16] M.R. Sturgeon, S. Kim, K. Lawrence, R.S. Paton, S.C. Chmely, M. Nimlos, T. D. Foust, G.T. Beckham, A mechanistic investigation of acid-catalyzed cleavage of aryl-ether linkages: implications for lignin depolymerization in acidic environments, ACS Sustain Chem. Eng. 2 (2014), https://doi.org/10.1021/sc400384w.

[17] R. Prado, A. Brandt, X. Erdocia, J. Hallet, T. Welton, J. Labidi, Lignin oxidation and depolymerisation in ionic liquids, Green Chem. 18 (2016), https://doi.org/10.1039/c5gc01950h.

[18] P.C. Rodrigues Pinto, E.A. Borges Da Silva, A.E. Rodrigues, Insights into oxidative conversion of lignin to high-added-value phenolic aldehydes, Ind. Eng. Chem. Res. 50 (2011) 741–748, https://doi.org/10.1021/ie102132a.

[19] M. Tayier, D. Duan, Y. Zhao, R. Ruan, Y. Wang, Y. Liu, Catalytic effects of various acids on microwave-assisted depolymerization of organosolv lignin, Bioresources 13 (2018) 412–424, https://doi.org/10.15376/biores.13.1.412-424.

[20] A. Rahimi, A. Ulbrich, J.J. Coon, S.S. Stahl, Formic-acid-induced depolymerization of oxidized lignin to aromatics, Nature 515 (2014) 249–252, https://doi.org/10.1038/nature13867.

[21] D.H. Patel, D. Marx, A.L.L. East, Improving the yield and rate of acid-catalyzed deconstruction of lignin by mechanochemical activation, ChemPhysChem 21 (2020), https://doi.org/10.1002/cphc.202000671.

[22] J.M. Nichols, L.M. Bishop, R.G. Bergman, J.A. Ellman, Catalytic C-O bond cleavage of 2-aryloxy-1-arylethanols and its application to the depolymerization of lignin-related polymers, J. Am. Chem. Soc. 132 (2010), https://doi.org/10.1021/ja106101f.

[23] M. Käldström, N. Meine, C. Farès, F. Schüth, R. Rinaldi, Deciphering "water-soluble lignocellulose" obtained by mechanocatalysis: new insights into the chemical processes leading to deep depolymerization, Green Chem. 16 (2014), https://doi.org/10.1039/c4gc00004h.

[24] N. Meine, R. Rinaldi, F. Schüth, Solvent-Free catalytic depolymerization of cellulose to water-soluble oligosaccharides, ChemSusChem 5 (2012), https://doi.org/10.1002/cssc.201100770.

[25] J. Kang, S. Irmak, M. Wilkins, Conversion of lignin into renewable carboxylic acid compounds by advanced oxidation processes, Renew. Energy 135 (2019) 951–962, https://doi.org/10.1016/j.renene.2018.12.076.

[26] R. Ma, Dicarboxylic Acids Platform Chemicals For Valorization Of Biorefinery Lignin (Doctoral thesis), Washington State University, 2016.

[27] S.K. Kansal, M. Singh, D. Sud, Studies on TiO_2/ZnO photocatalysed degradation of lignin, J. Hazard. Mater. 153 (2008) 412–417, https://doi.org/10.1016/j.jhazmat.2007.08.091.

[28] B. Neppolian, H.C. Choi, M.V. Shankar, B. Arabindoo, V. Murugesan, Semiconductor-assisted photodegradation of textile dye, reactive red 2 by ZnO in aqueous solution, in: Proceedings of the International Symposium on Environmental Pollution Control and Waste Management, Tunis, 2002, 647–653.

[29] Z. Du, W. Li, Z. Xu, H. Wu, H. Jameel, H.M. Chang, L.L. Ma, Characterization Of C60/Bi2TiO4F2 as a potential visible spectrum photocatalyst for the depolymerization of lignin, J. Wood Chem. Technol. 36 (2016) 365–376, https://doi.org/10.1080/02773813.2016.1173063.

[30] J.D. Nguyen, B.S. Matsuura, C.R.J. Stephenson, A photochemical strategy for lignin degradation at room temperature, J. Am. Chem. Soc. 136 (2014) 1218–1221, https://doi.org/10.1021/ja4113462.

[31] J. Gong, A. Imbault, R. Farnood, The promoting role of bismuth for the enhanced photocatalytic oxidation of lignin on Pt-TiO_2 under solar light illumination, Appl. Catal. B 204 (2017) 296–303, https://doi.org/10.1016/j.apcatb.2016.11.045.

[32] M.A. Lazar, S. Varghese, S.S. Nair, Photocatalytic water treatment by titanium dioxide: recent updates, Catalysts 2 (2012) 572–601, https://doi.org/10.3390/catal2040572.

[33] L. Rideh, A. Wehrer, D. Ronze, A. Zoulalian, Photocatalytic degradation of 2-chlorophenol in TiO_2 aqueous suspension: modeling of reaction rate, Ind. Eng. Chem. Res. 36 (1997) 4712–4718, https://doi.org/10.1021/ie970100m.

[34] S. Totong, P. Daorattanachai, A.T. Quitain, T. Kida, N. Laosiripojana, Catalytic depolymerization of alkaline lignin into phenolic-based compounds over metal-free carbon-based catalysts, Ind. Eng. Chem. Res. 58 (2019), https://doi.org/10.1021/acs.iecr.9b01973.

[35] A. Ahlbom, M. Maschietti, R. Nielsen, M. Hasani, H. Theliander, Towards understanding kraft lignin depolymerisation under hydrothermal conditions, Holzforschung 76 (2021), https://doi.org/10.1515/hf-2021-0121.

[36] K. Hofstadler, R. Bauer, S. Novallc, G. Heisler, New reactor design for photocatalytic wastewater treatment with TiO_2 immobilized on fused-silica glass fibers: photomineralization of 4-chlorophenol, Environ. Sci. Technol. 28 (1994) 670–674, https://doi.org/10.1021/es00053a021.

[37] J. Villaseñor, H.D. Mansilla, Effect of temperature on kraft black liquor degradation by ZnO-photoassisted catalysis, J. Photochem. Photobiol. A Chem. 93 (1996), https://doi.org/10.1016/1010-6030(95)04179-6.

[38] J. Kou, C. Lu, J. Wang, Y. Chen, Z. Xu, R.S. Varma, Selectivity enhancement in heterogeneous photocatalytic transformations, Chem. Rev. 117 (2017) 1445–1514, https://doi.org/10.1021/acs.chemrev.6b00396.

[39] C. Awungacha Lekelefac, N. Busse, M. Herrenbauer, P. Czermak, Photocatalytic based degradation processes of lignin derivatives, Int. J. Photoenergy 2015 (2015), https://doi.org/10.1155/2015/137634.

[40] H. Lempiäinen, K. Lappalainen, M. Mikola, T. Tuuttila, T. Hu, U. Lassi, Acid-catalyzed mechanocatalytic pretreatment to improve sugar release from birch sawdust: structural and chemical aspects, Catal. Today (2022) 397–399, https://doi.org/10.1016/j.cattod.2021.06.015.

[41] M. Havimo, P. Hari, Temperature gradient in wood during grinding, Appl. Math. Model 34 (2010), https://doi.org/10.1016/j.apm.2009.12.021.

[42] C. Zhang, L.H. Xu, C.Y. Ma, H.M. Wang, Y.Y. Zhao, Y.Y. Wu, J.L. Wen, Understanding the structural changes of lignin macromolecules from balsa wood at different growth stages, Front. Energy Res. 8 (2020) 1–9, https://doi.org/10.3389/fenrg.2020.00181.

[43] A. Fujimoto, Y. Matsumoto, H.M. Chang, G. Meshitsuka, Quantitative evaluation of milling effects on lignin structure during the isolation process of milled wood lignin, J. Wood Sci. 51 (2005) 89–91, https://doi.org/10.1007/s10086-004-0682-7.

[44] S.G. Yao, J.K. Mobley, J. Ralph, M. Crocker, S. Parkin, J.P. Selegue, M.S. Meier, Mechanochemical treatment facilitates two-step oxidative depolymerization of Kraft lignin, ACS Sustain. Chem. Eng. 6 (2018) 5990–5998, https://doi.org/10.1021/acssuschemeng.7b04597.

[45] Z. Huang, N. Luo, C. Zhang, F. Wang, Radical generation and fate control for photocatalytic biomass conversion, Nat. Rev. Chem. 6 (2022), https://doi.org/10.1038/s41570-022-00359-9.